frontiers | Frontiers in Marine Science

TYPE Original Research
PUBLISHED 21 February 2023
DOI 10.3389/fmars.2023.1144818

OPEN ACCESS

EDITED BY
Jiapeng Wu,
Guangzhou University, China

REVIEWED BY
Dewang Li,
Ministry of Natural Resources, China
Guo Wei,
East China University of Technology, China
Dongliang Lu,
Beibu Gulf University, China

*CORRESPONDENCE
Fajin Chen
fjchen@gdou.edu.cn

SPECIALTY SECTION
This article was submitted to Marine Biogeochemistry, a section of the journal Frontiers in Marine Science

RECEIVED 15 January 2023
ACCEPTED 09 February 2023
PUBLISHED 21 February 2023

CITATION
Lu X, Wang C, Lao Q, Jin G, Chen F, Zhou X and Chen C (2023) Interactions between particulate organic matter and dissolved organic matter in a weak dynamic bay revealed by stable isotopes and optical properties.
Front. Mar. Sci. 10:1144818.
doi: 10.3389/fmars.2023.1144818

Interactions between particulate organic matter and dissolved organic matter in a weak dynamic bay revealed by stable isotopes and optical properties

Xuan Lu[1,2,3], Chao Wang[1,2,3], Qibin Lao[1,2,3], Guangzhe Jin[1,2,3], Fajin Chen[1,2,3]*, Xin Zhou[1,2,3] and Chunqing Chen[1,2,3]

[1]College of Ocean and Meteorology, Guangdong Ocean University, Zhanjiang, China, [2]Key Laboratory for Coastal Ocean Variation and Disaster Prediction, Guangdong Ocean University, Zhanjiang, China, [3]Key Laboratory of Climate, Resources and Environment in Continental Shelf Sea and Deep Sea of Department of Education of Guangdong Province, Guangdong Ocean University, Zhanjiang, China

Few studies have incorporated the tools of stable isotopes and optical properties to study the biogeochemical process of organic matter (OM), including particulate organic matter (POM) and dissolved organic matter (DOM), which prevents our comprehension of the interactions between POM and DOM in the marine environment. In this study, the origin, distribution, and fate of POM and DOM in Tieshangang Bay, a weak dynamic bay were investigated by measuring $\delta^{13}C$ and $\delta^{15}N$ of POM, dissolved organic carbon (DOC), and absorption and fluorescence of DOM (CDOM and FDOM). In the upper bay, POM source was mainly originated from terrestrial discharge, whereas the high fluorescence index (FI) indicated that external aquatic organism activity dominated DOM sources. In contrast, in the outer bay, the slightly increased $\delta^{13}C$ and enriched $\delta^{15}N$ of POM and enhanced fluorescence intensities of protein-like DOM components indicated the considerable contributions of the *in situ* biological activities to OM. A net addition of DOC and optical components of DOM occurred in both the upper and outer bays. The decomposition of terrestrial POM was responsible for the addition of DOM due to the weak dynamics in the upper bay, whereas the enhanced primary production and the strong decomposition of freshly produced POM jointly contributed to the addition of DOM in the outer bay. Our study suggests that hydrodynamics regulate the biogeochemistry and interactions of POM and DOM in the weak dynamic bay.

KEYWORDS

biogeochemistry, particulate organic matter, dissolved organic matter, isotopic and optical analyses, Beibu Gulf

1 Introduction

Estuaries and coastal bays are transitional areas from terrestrial to oceanic ecosystems with typically complicated environments (Lin et al., 2019; He et al., 2022a). An estimated 0.5 Pg C of organic carbon (OC) was transported from rivers to the oceans each year (Bianchi, 2011; Gao et al., 2021a), and more than 90% OC is buried in coastal area (Huang et al., 2020). Thus, the dynamics of organic matter (OM), including particulate organic matter (POM) and dissolved organic matter (DOM) in the estuaries and coastal bays, are important for the global matter cycle and climate change (Tremblay et al., 2015; Karlsson et al., 2016; Qu et al., 2022).

However, the behavior of OM in estuaries and coastal bays is complicated due to the OM is supplied from multiple sources, including terrestrial plant detritus, soils, *in-situ* aquatic production and exogenous offshore marine environments sources (Ke et al., 2020; Samantaray and Sanyal, 2022; Akcay et al., 2022). Moreover, due to the complex hydrological conditions in the estuaries and bays, the OM dynamics in estuaries and bays are subject to high spatial and temporal variability (Liu et al., 2020a; Chen et al., 2021). In addition, the heterotrophy in the coastal oceans may increase the release of carbon dioxide (CO_2) by the decomposition (Blair and Aller, 2012; Sarma et al., 2014; Gao et al., 2021b). Previous studies also suggested that ~35% of the POM is labile and easily degraded by the microorganisms (Hedges et al., 1997; Sarma et al., 2014; Ye et al., 2017). Therefore, a systematic understanding of the origin, distribution, and sink of OM in estuaries and bays is essential (Gao et al., 2021a; Samantaray and Sanyal, 2022; Dan et al., 2022).

Stable isotopic compositions ($\delta^{13}C$ and $\delta^{15}N$) of POM and the geochemical indicators (i.e., C/N ratio of the POM) are considered as useful tools to discriminate the source and sink of POM in marine environments. (Chen et al., 2021; Dan et al., 2022; Xia et al., 2022). For instance, the $\delta^{13}C$ compositions of POM from terrestrial sources (-30‰ to -23‰) are different from marine sources (-22‰ to -19‰) (Meyers, 1994; Meyers, 1997). Similarly, the $\delta^{15}N$ compositions of terrestrial vascular plants (-5‰ to 18‰) are higher than that of the marine OM (3‰ to 12‰) (Wada & Hattori, 1990). Additionally, the C/N ratios of POM can be used to identify the marine sources (5-8) and terrestrial source (≥20) (Meyers, 1997). In addition, in recent years, spectroscopic techniques have been used to assess its distribution, source and fate at land–sea interfaces (Chen et al., 2022b; Qu et al., 2022; Sun et al., 2022). For example, the absorption coefficients of certain wavelengths (e.g., 254 nm, 325 nm) can be regarded as the levels of chromophoric dissolved organic matter (CDOM). In addition, the spectral slopes (e.g., $S_{275\text{-}295}$) and specific UV absorbance (e.g., $SUVA_{254}$) are considered as reliable qualitative indices for the DOM molecular size and its aromaticity (Weishaar et al., 2003; Wang et al., 2021b; Sun et al., 2022). A small portion of CDOM is defined as fluorescent DOM (FDOM). The FDOM spectrum can be used to describe DOM quantity (i.e., intensities of various fluorescent components) (Chen et al., 2022b; Sun et al., 2022) and quality (i.e., humification index (HIX), biological index (BIX) and fluorescence index (FI)) (Stedmon & Bro, 2008; Huguet et al., 2009; Li et al., 2022b). The variations of these spectroscopic indices in the land–sea interface were also obvious (Gao et al., 2019; Sun et al., 2022), which can be applied to identify the anthropogenic and natural sources (Liu et al., 2020b; Li et al., 2022b), biogeochemical behaviors (Li et al., 2022a) and export fluxes, and responses to climate changes for DOM in these dynamic systems (Qu et al., 2020). The source and distribution of POM or DOM have been studied in some areas around the world (Kaiser et al., 2013; Liu et al., 2020a; Chen et al., 2021). However, to date, few studies have incorporated stable isotopes and optical properties to systematically explore the sources, biogeochemical behaviors and interactions of OM in water environment (Qu et al., 2022).

The Beibu Gulf is located in the northern South China Sea (NSCS), and is a newly emerging industrial region in China. Multiple water masses influence the Beibu Gulf and carry stable external nutrient and other materials into the Beibu gulf to sustain marine production (Lao et al., 2022). Thus, the Beibu Gulf is generally characterized with high productivity and rich biodiversity, and is becoming an important mariculture base and fishing ground (Xu et al., 2020; Lin et al., 2021). However, environmental contamination in the gulf have gradually increased over the past decades because anthropogenic activities such as sewage treatment, coastal aquaculture, industrial runoff, and agriculture have intensively accelerated nutrient inputs to Beibu Gulf coastal ecosystems, especially in the rainy season (Xu et al., 2021; Zhu et al., 2022). Tieshangang Bay is a weak dynamic process bay in northeastern Beibu Gulf due to no large river input, and the tide is the main factor influencing water exchange in the bay (Jiang et al., 2017). Tieshangang Bay is a representative coastal bay of Guangxi Province. The rapid industrialization and urbanization have caused serious pollution around the coastal area in the bay (Lao et al., 2022). Compared with large catchments, the seasonal variation and anthropogenic activities have more great impacts on the coastal bays (such as Tieshangang Bay) (Zhang et al., 2019; Zhao et al., 2021). Therefore, Tieshangang Bay is an ideal area to explore OM dynamics under the influences of the increasing land-based input during the rainy seasons.

In this study, POC, PN, $\delta^{13}C$, and $\delta^{15}N$ of POM, DOC, CDOM and FDOM, associated with hydrological and environmental parameters, such as temperature, salinity, apparent oxygen utilization (AOU), nutrients (NH_4^+, NO_2^-, NO_3^-, PO_4^{3-}) and chlorophyll-a (Chl *a*) were analyzed in Tieshangang Bay. We attempted to comprehensively understand the sources, distributions and interactions of POM and DOM, to quantify the connections between the POM and DOM, and to discuss the biogeochemical process of OM in the Tieshangang Bay.

2 Materials and methods

2.1 Study region

The Beibu Gulf is in the NSCS (Figure 1), covering an area of ~12.8×10^4 km^2. Tieshangang Bay (109°26′ - 109°45′E; 21°28′-21° 45′ N) is one of the most industrial and harbor bay in the Beibu Gulf. Due to a combination of semi-enclosed topographic restrictions, lack of riverine input, weak local sea currents, and

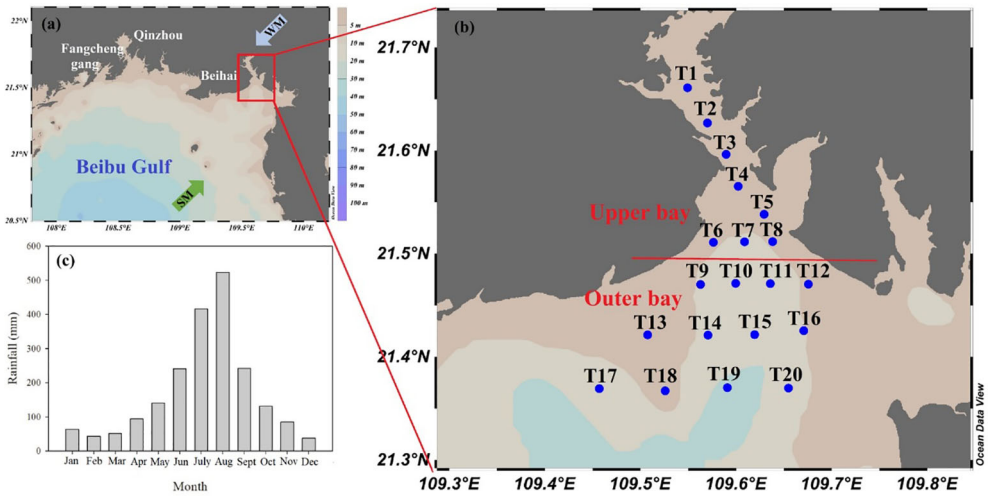

FIGURE 1
(A) Study location. WM, winter monsoon; SM, summer monsoon. **(B)** sampling sites in Tieshangang Bay, and **(C)** mean monthly rainfall (mm) from 2012-2021 in Beihai city. (https://en.tutiempo.net/) .

diurnal tides, Tieshangang Bay has a low water exchange rate (Jiang et al., 2017). Moreover, the average water residence time in the Tieshangang Bay is 64.0 days (Pei et al., 2019). Recently, human activities, including industry, agriculture and fishing, have a significant impact on the ecological environment of the bay (Chen et al., 2022a; Gan et al., 2013). Additionally, Tieshangang Bay is affected by monsoon. The rainfall is heavy (~86% of the total) from April to October (wet season), which is much higher than that from the November to March of following year (dry season) (Figure 1C).

2.2 Sampling collection

The cruise with 20 stations was conducted in Tieshangang Bay during the early rainy season (March 31 - April 1, 2021). At each station, surface samples (at 0.5-m depth) and bottom samples (when the depth >10 m) were collected. However, the study only shows the picture of the surface layer due to the number of bottom samples is rare. To meet the needs of our study, based on the characteristics of hydrological and environmental parameters, stable isotope and optical properties, the study area was classified into two regions: the upper bay (Stations T1-T8) and the outer bay (Stations T9-T20) (Figure 1) (Chen et al., 2022a). Seawater samples were collected on the deck. The seawater samples were filtered using acid-cleaned 0.45-μm acetate cellulose filters and then stored at -20° C for nutrient measurement. Approximately 500 ml seawater was passed through a glass fiber membrane (47-mm, GF/F, Whatman) and then cryopreservation (-20°C) for postcruise Chl *a* analysis in the laboratory. Preweighed and precombusted 47-mm diameter filters (GF/F, Whatman) were used to collect POM (POC and PN), and the POM samples were cryo-preserved (-20°C) before analysis. Water samples for DOM analysis, including DOC, CDOM and FDOM, were filtered immediately using precleaned 0.45-μm pore cellulose acetate filters, and the filtrates were stored in high-density polyethylene (HDPE) vials at -20°C and dark condition before further treatment.

2.3 Measurements of DO, nutrients, Chl *a* and DOC

In the laboratory, the iodometric method was used to measure DO. Nutrient sample for the analysis of NO_3^-, NO_2^-, and PO_4^{3-}, was measured by a San^{++} continuous flow analyzer (Skalar, Netherlands). The seawater sample for NH_4^+ was measured using spectrophotometry. 90% acetone was added to extract the Chl *a* from the GF/F filter, and the fluorometric method were used to obtain the Chl *a* (Lorenzen, 1967). The DOC concentrations were analyzed by the vario TOC analyzer (Elementar, Germany) under high-temperature (680°C) catalytic oxidation mode. DOC concentrations were obtained by potassium hydrogen phthalate standards. The reproducibility of duplicate measurement for DOC analysis was 2%.

2.4 TSM, POC, PN and isotope analyses

The concentrations of total suspended matter (TSM) were measured from the weight of suspended sediment in filter by the volume of water. For POC and PN, the dried filters were placed in the bottle containing concentrated HCl vapor for decarbonation, and then washed using deionized water and dried at 50°C for two days (48 h). Then, the treated filters were introduced into an elemental analysis isotope ratio mass spectrometer (MAT 253 plus, EA-IRMS) for the analysis of POC and PN. The average standard deviation for $\delta^{13}C$ and $\delta^{15}N$ were all ±0.2‰, and for the contents of POC and PN were all ±0.1%.

2.5 CDOM analysis

Shimadzu UV-1780 dual beam spectrophotometer (Shimadzu, Japan) with 10-cm quartz cells was used to determine the CDOM absorbance spectra. Absorbance (A_λ) was obtained from wavelengths 240 and 800 nm at 0.5 nm intervals. The a_λ (CDOM Napierian absorption coefficient, m^{-1}) was calculated according to 2.303 times absorbance at wavelength λ (A_λ) divided by the light pathlength of the cell in meters (0.1 m). In this study, a_{254} and a_{325} and were used to quantify CDOM. (Wang et al., 2021a). Other popular wavelengths (e.g., 280 nm, 350 nm, 355 nm, 412 nm) of the CDOM absorption coefficients are presented in Table S1 to facilitate comparisons among different studies. The $S_{275\text{-}295}$ is a spectral slope between 275-295 nm, as an indicator of the relative molecular weight of DOM (Helms et al., 2008). The index for DOM aromaticity ($SUVA_{254}$, mg C L^{-1}) was calculated as decadal absorption coefficient (i.e., A(λ)/L) divided by the DOC concentration (Wang et al., 2021b).

2.6 FDOM analysis and PARAFAC modeling

The fluorescence spectrofluorometer (Hitachi F-7100, Japan) fitted with a 1-cm quartz cuvette was used to acquire the FDOM excitation-emission matrices (EEMs). The excitation (Ex) wavelengths spanned at 240-450 nm in 5 nm increments, and emission (Em) wavelengths spanned at 280-600 nm in 2 nm increments. The slit widths of emission and excitation were set to 5 nm and 10 nm, respectively. The fluorescence intensities are present in Raman units (R.U. nm^{-1}). HIX was used to identify the DOM humification degree (Zsolnay et al., 1999). BIX is used to indicate the new generated DOM in aquatic ecosystems (Huguet et al., 2009). FI is calculated to trace DOM sources (Cory and Mcknight, 2005). FI value > 1.9 denotes biological source of DOM, and the FI value<1.4 denotes the dominant terrestrial sources (Li et al., 2022b).

In this study, two humic-like components (C1: Ex/Em, ≤ 240, 290/390 nm, included peaks A and M; C2: Ex/Em, 260,360/440 nm, included peaks A and C) (Coble, 1996) and one protein-like component (C3: Ex/Em, 275/328 nm, peak T) (Coble, 1996) were identified in this study (Figure S1).

2.7 Two end-member mixing model

Salinity is one of the most important conservative parameters in seawater, a two end-member mixing model (the upper bay and outer bay end-member) was established in Tieshangang Bay to assess the biogeochemical behaviors of nutrients, DOC, CDOM and FDOM. For a discussion of nutrients, DOC, CDOM and FDOM sources and dynamics, in this study, because fluorescence intensities in T1 were no data, we selected the Station T2 water (salinity = 31.19) and the T18 water (salinity = 31.82) as the two end-members, respectively. The values of salinity, nutrients, DOC, CDOM and FDOM for the two end-members are shown in Table 1.

The salinity in each sample from Tieshangang Bay can be expected to follow Equations (1)-(2):

$$f_u + f_o = 1 \tag{1}$$

$$f_u Sal_u + f_o Sal_o = Sal \tag{2}$$

where f_u and f_o represent the fractions of the upper bay end-member and outer bay end-member in the sample, respectively. Based on the measured end-member values of nutrients, DOC, CDOM and FDOM (Table 1), the net-conservative changes (ΔN) in nutrients, DOC, CDOM and FDOM for a given sample can be calculated by subtracting its theoretical conservative mixing values as follows:

$$\Delta N = N - f_u N_u - f_o N_o \tag{3}$$

where N denotes nutrients, DOC, CDOM or FDOM. Positive or negative ΔN values denote biogeochemical addition or removal processes during water mass mixing in Tieshangang Bay.

To further assess the robustness of this model and their derived net DOM values, we performed a perturbation test (Lønborg and Álvarez-Salgado, 2014). Here we assumed the salinity of two end-members fluctuates in the range of ±5%. For simplicity, a total of 50 perturbations test were conducted for the DOC. The valid tests showed the consistent results to the initial model (i.e., net addition of DOC with 0.14 ± 0.12 mg L^{-1}) and demonstrated the robustness of this model.

2.8 Bayesian mixing model

The Bayesian mixing model is used for quantification of potential POM sources in the Tieshanggang Bay in R software (MixSIAR v.3.1.10) (Chen et al., 2021), and the framework can be found in Supporting Information Text S1. The details of this model can be found in Lao et al. (2019). In addition, previous studies have shown that the Bayesian mixture models can be

TABLE 1 The chemical properties for the upper bay and outer bay end-members.

End-member	Salinity	DOC (mg L^{-1})	a_{254} (m^{-1})	a_{325} (m^{-1})	C1(10^{-2} RU)	C2(10^{-2} RU)	C3(10^{-2} RU)	NH_4^+ (μmolL^{-1})	NO_2^- (μmol L^{-1})	NO_3^- (μmol L^{-1})	PO_4^{3-} (μmol L^{-1})
Upper bay	31.19	64.17	3.27	0.88	10.75	7.52	4.99	2.31	0.92	7.21	0.80
Outer bay	31.82	38.33	1.66	0.41	5.49	2.63	4.47	0.84	0.20	0.36	0.08

applied to quantify the origin of POM since different POM have different isotopic signatures (Kubo and Kanda, 2016; Chen et al., 2021).

2.9 Statistical analysis

The correlation analysis of different parameters and analysis of Student's *t*-test of the difference between the parameters in the two groups were analyzed using SPSS 22.0.

3 Results

3.1 Physiochemical parameters

Figure 2 presents the basic physiochemical parameters for this cruise (Chen et al., 2022a). The temperature in the seawater ranged from 24.0 to 27.3°C (25.3 ± 0.68°C average). Salinity in the seawater ranged from 30.59 to 31.82 (with an average of 31.55 ± 0.27). The salinity increased seaward indicating that it is influenced by coastal freshwater discharge. AOU values were in the range of -0.97 and

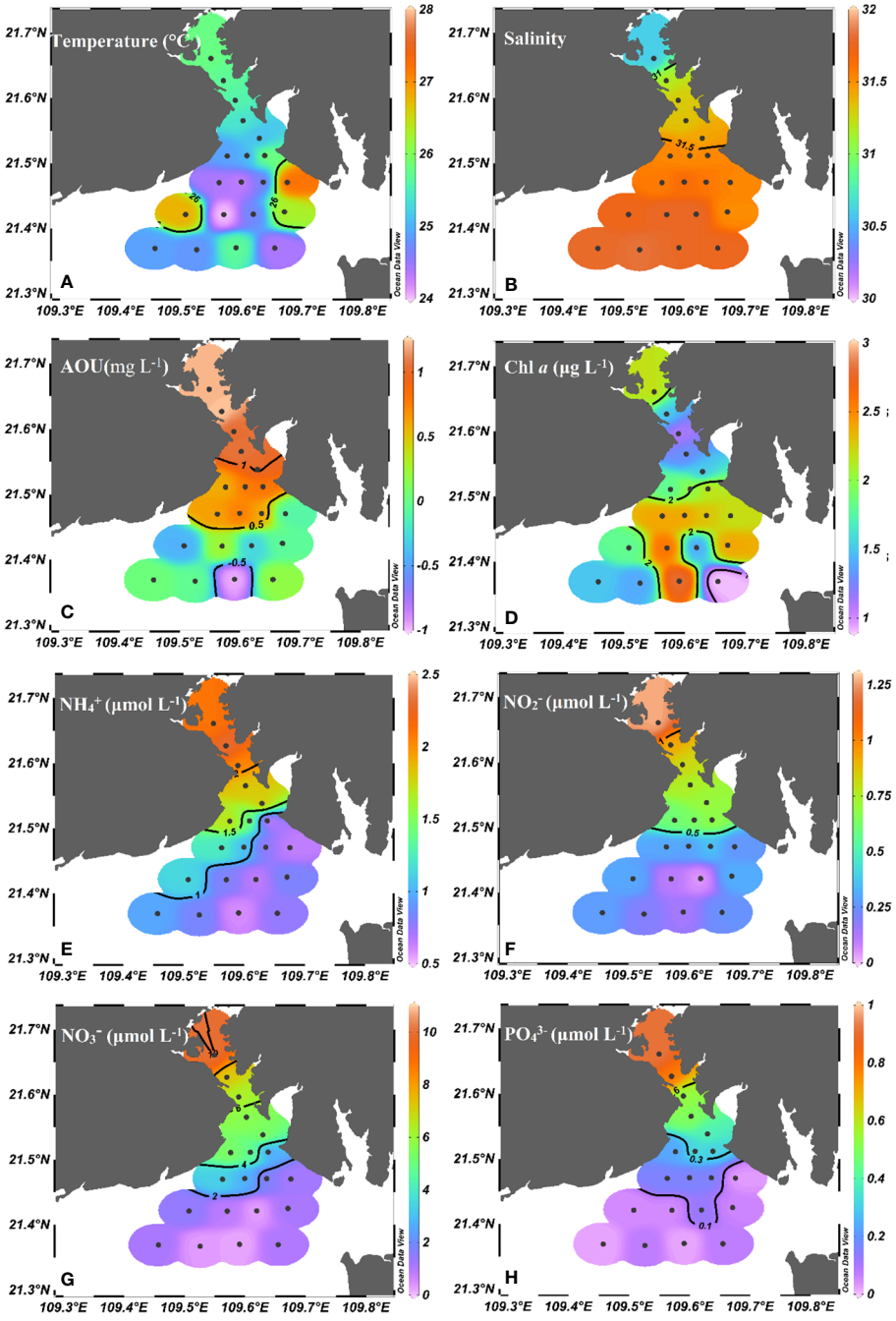

FIGURE 2
Spatial variations of **(A)** temperature, **(B)** salinity, **(C)** AOU, **(D)** Chl a, and nutrients [**(E)** NH_4^+, **(F)** NO_2^-, **(G)** NO_3^-, **(H)** PO_4^{3-}] in Tieshangang Bay. Black dots donate sampling sites.

1.25 mg L^{-1}(averaged at 0.42 ± 0.61 mg L^{-1}), showing a decreasing tendency seaward. The Chl *a* concentration ranged from 0.90-2.80 μg L^{-1} (averaged at 1.75 ± 0.53 μg L^{-1}) and showed high values in the outer bay. Obviously, nutrients (NH_4^+, NO_2^-, NO_3^-, PO_4^{3-}) were decreased seaward. The NH_4^+, NO_2^-, NO_3^- and PO_4^{3-} concentrations ranged from 0.60 to 2.31 μmol L^{-1} (1.26 ± 0.58 μmol L^{-1}average), 0.05 to 1.28 μmol L^{-1} (0.46 ± 0.31 μmol L^{-1} average), 0.23 to 10.07 μmol L^{-1} (3.27 ± 2.70 μmol L^{-1}average) and 0.02 to 0.92 μmol L^{-1} (0.25 ± 0.25 μmol L^{-1}average), respectively. Notably, NO_3^- is the dominant DIN in Tieshangang Bay.

3.2 POC, PN, TSM, C/N ratios, $\delta^{13}C$, and $\delta^{15}N$

The concentrations of POC and PN ranged from 0.38-0.82 mg L^{-1} (0.49 ± 0.11 mg L^{-1}average) and from 0.03 mg L^{-1} to 0.09 mg L^{-1} (0.05 ± 0.01 mg L^{-1}average), respectively. Generally, higher POC and PN concentrations were found in T8 and T19 in the outer bay (Figure 3). In addition, POC% and PN% in TSM varied between 1.49% and 4.92% (2.31 ± 0.72% average), 0.14% and 0.42% (0.23 ± 0.07% average), respectively.

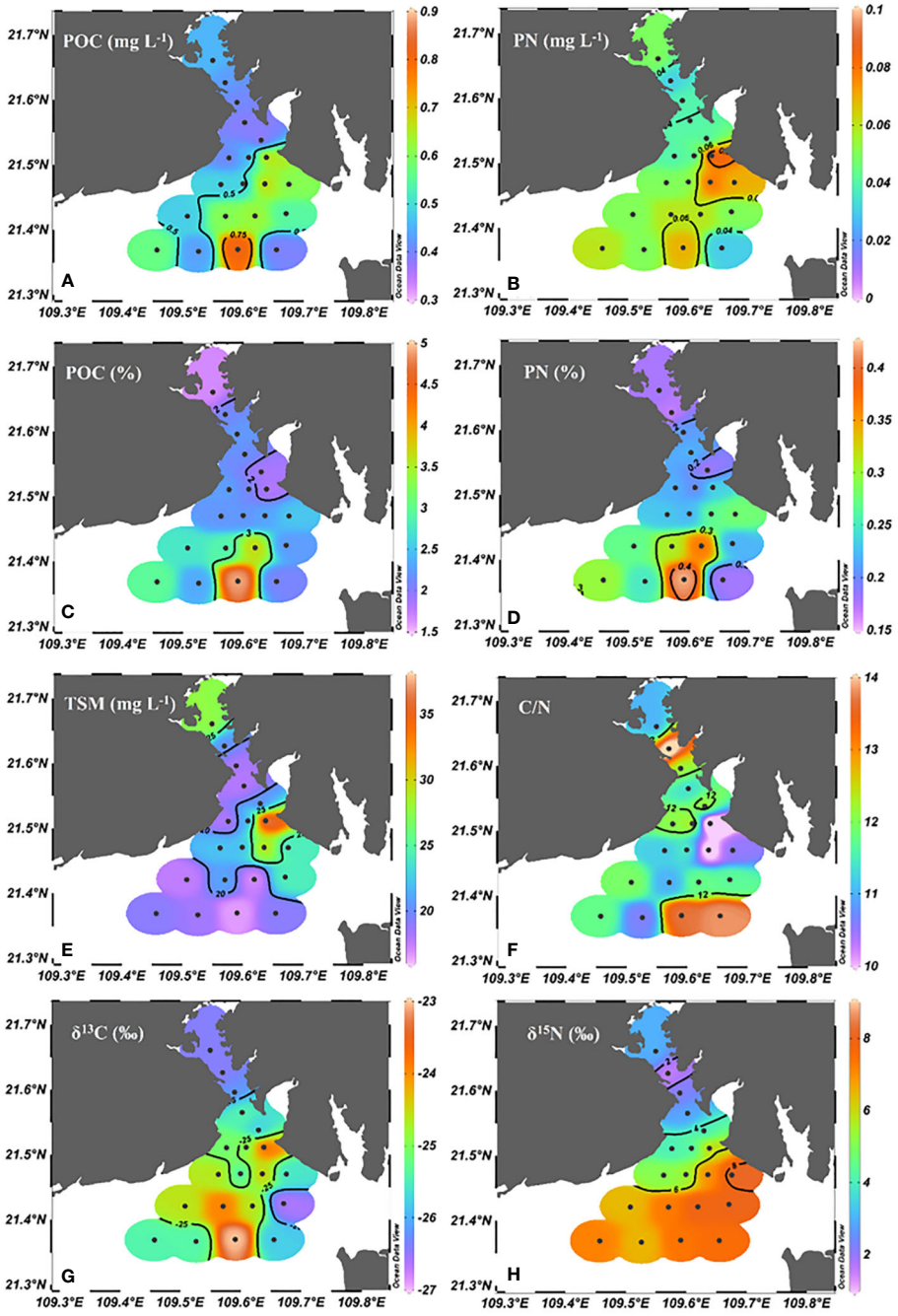

FIGURE 3
Spatial variations of **(A)** POC, **(B)** PN, **(C)** POC%, **(D)** PN%, **(E)** TSM, **(F)** C/N, **(G)** $\delta^{13}C$ **(H)** $\delta^{15}N$ in Tieshangang Bay. Black dots are sampling sites.

The TSM concentration ranged from 16.60 to 37.60 mg L^{-1} (averaged at 22.12 ± 4.95 mg L^{-1}), and the highest concentration was found in the upper bay (T8). The C/N values varied between 9.8-13.2 (11.90 ± 1.33 average) and presented a fluctuation across the bay. The $\delta^{13}C$ values varied from -26.6‰ to -23.0‰ (averaged at -25.3 ± 0.9‰) and increased seaward. The $\delta^{15}N$ values ranged from 1.5‰ to 8.1‰ (5.5 ± 2.0‰ average) and increased seaward (Figure 3).

3.3 Distributions of DOC, CDOM and FDOM

The distributions of DOC, CDOM and FDOM parameters are shown in Figures 4, 5. The concentrations of DOC ranged from 0.38 to 1.25 mg L^{-1}, averaged at 0.77 ± 0.23 mg L^{-1}. The highest DOC concentrations were observed at Station T9, while lower DOC concentrations were observed at Stations T11, T18 and T20. Interestingly, DOC concentrations were nearly homogeneous in the upper bay. The CDOM absorption coefficient at 254 nm (a_{254}) ranged from 1.73 to 5.64 m^{-1} in the waters of Tieshangang Bay, averaged at 2.87 ± 0.78 m^{-1} (Figure 4A). Generally, the a_{254} value decreased seaward. The CDOM absorption coefficients at five longer wavelengths (a_{280}, a_{325}, a_{350}, a_{355}, a_{412}) show significant positive relation ($p< 0.01$, n = 26). Therefore, for simplicity, we report only the a_{325} result. The a_{325} value ranged from 0.41 to 1.50 m^{-1}, averaged at 0.72 ± 0.21 m^{-1}. a_{325} were a significantly correlated with a_{254} ($R^2 = 0.96$, $p< 0.01$, n = 26) and had a similar distribution pattern of a_{254} in Tieshangang Bay (Figure 4C). The spectral slope $S_{275\text{-}295}$ (20.9-24.2 μm^{-1}) showed a contrasting spatial pattern with a_{254} and a_{325} (Figure 4D). A higher average value of $S_{275\text{-}295}$ was obtained in the outer bay than in the upper bay (t-test, $p< 0.001$). The $SUVA_{254}$ ranged from 1.16 to 2.66 $m^2\ g^{-1}$ C, averaged at 1.70 ± 0.44, and the highest $SUVA_{254}$ occurred in T1 (Figure 4E).

The humic-like C1 and C2 fluorescence intensity ranged from 5.62×10^{-2} to 13.80×10^{-2} RU and 2.80×10^{-2} to 9.00×10^{-2} RU, respectively, and they were correlated significantly ($R^2 = 0.97$, $p< 0.01$, n = 25). Except for two unusually high values on the west side of the

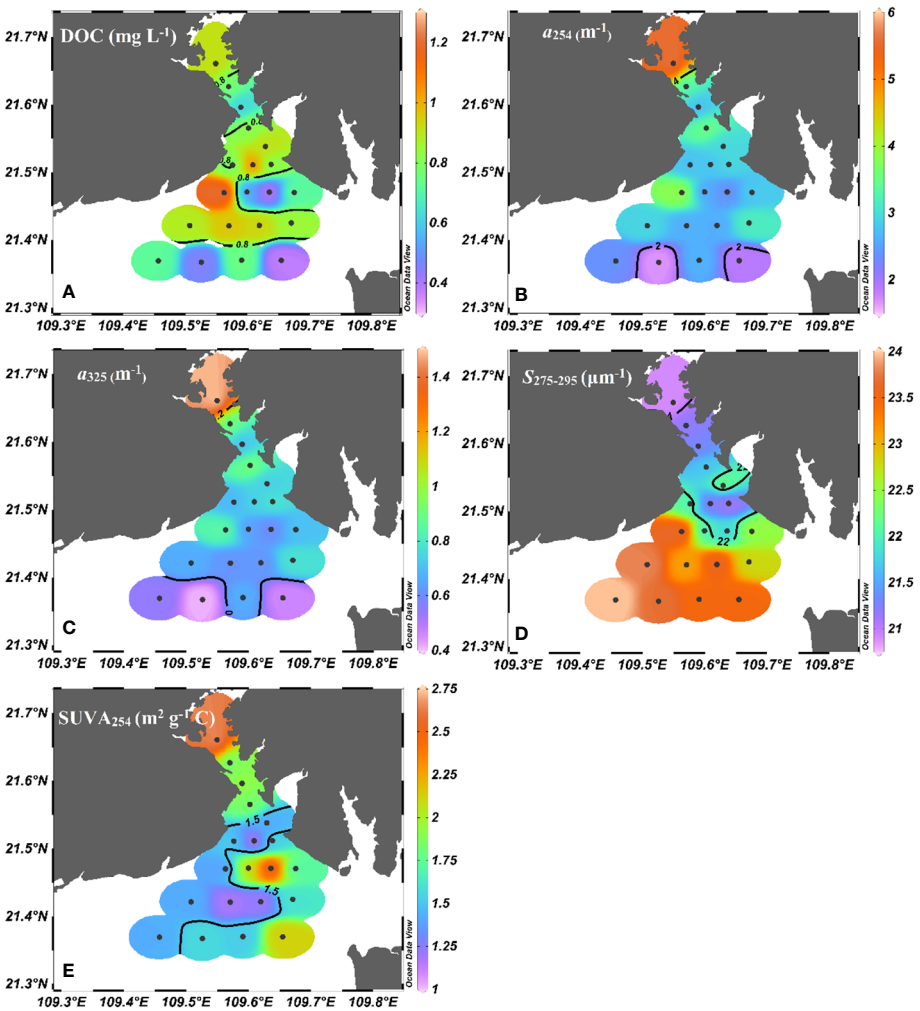

FIGURE 4
Spatial variations of **(A)** DOC (mg L^{-1}), **(B)** a_{254} (m^{-1}), **(C)** a_{325} (m^{-1}), **(D)** $S_{275\text{-}295}$ (μm^{-1}), and **(E)** $SUVA_{254}$ ($m^2\ g^{-1}$ C) in Tieshangang Bay. Black dots are sampling sites.

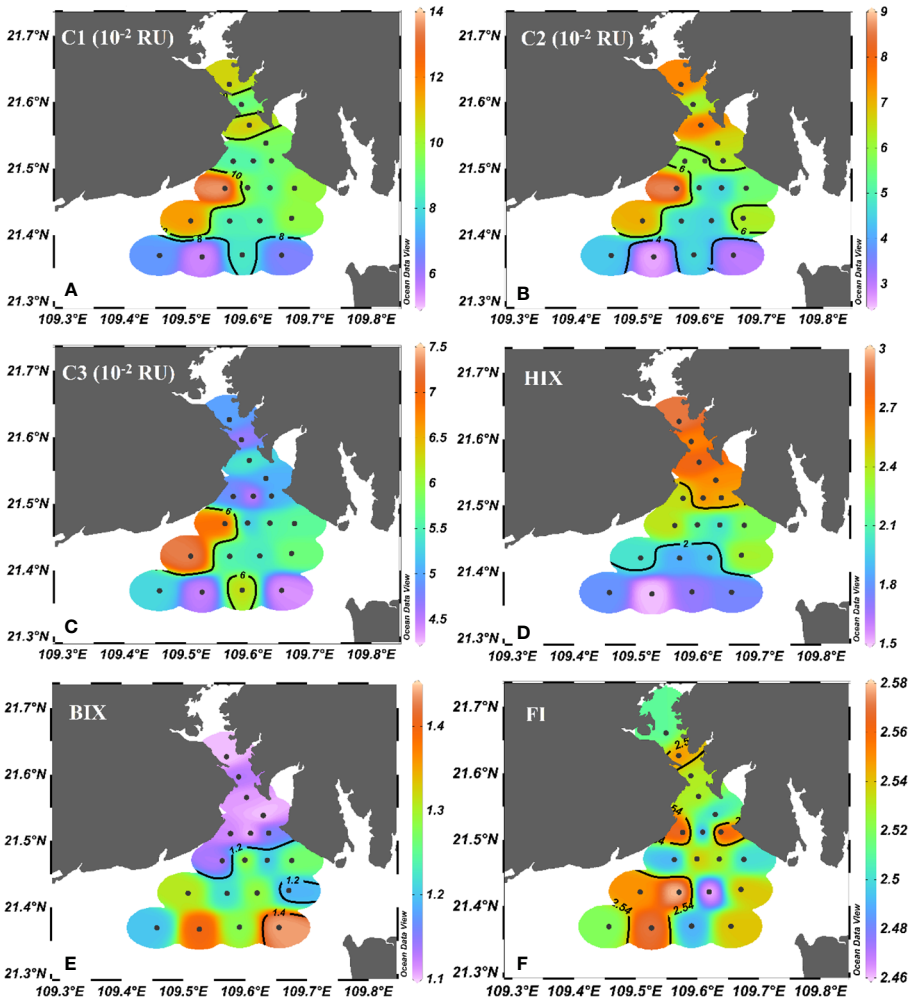

FIGURE 5
Spatial variations of **(A)** C1 (10^{-2} RU), **(B)** C2 (10^{-2} RU), **(C)** C3 (10^{-2} RU), **(D)** HIX and **(E)** BIX, **(F)** FI in Tieshangang Bay. Black dots denote sampling sites.

outer bay (T9 and T13), the fluorescence intensities of humic-like C1 and C2 substantially decreased seaward (Figures 5A, B). The intensity of protein-like C3 were in the range of 4.39 × 10^{-2} to 7.28 ×10^{-2} RU. The C3 intensity was low and nearly homogeneous in the upper bay (average 5.44 ± 0.73 ×10^{-2} RU), whereas it varied much more in the outer bay, with a high value point on the west side (T13) and a low value point on the south side (T20) (Figure 5C). HIX varied from 1.38 to 2.96 and generally decreased seaward (Figure 5D). By contrast, BIX varied from 1.10 to 1.54 and showed the opposite distribution pattern to HIX (Figure 5E). The FI varied from 2.46 to 2.64 and showed a slight fluctuation in Tieshangang Bay (Figure 5F).

4 Discussion

4.1 Different sources of POM in the upper and outer bays

Bulk POM at the upper stations showed lower POC (0.45 ± 0.08 mg L^{-1}) and PN (0.05 ± 0.02 mg L^{-1}) contents than those at the outer stations (Figure 3 and Table 2). A strong correlation between POC concentration versus PN concentration in the upper bay (p< 0.01, n= 11) demonstrated similar sources of the two components (Figure S2). In addition, the C/N was up to ~12 in the upper bay, together with more depleted $\delta^{13}C$ (-25.3‰) and $\delta^{15}N$ (3.6‰) (Table 2 and Figure 6), suggesting that the POM (Table 2 and Figure 6E) primarily comes from terrestrial sources. The lower POC% and PN% of TSM also suggested that more terrestrial sources contribute to POM in the upper bay (Table 1). Therefore, this region is dominated by the terrestrial POM (Guo et al., 2015; Chen et al., 2020). Generally, terrestrial organic matter (i.e., soil OM, sewage, C3 and C4 plants), freshwater phytoplankton and marine organic matter are potential contributions to POM. The $\delta^{13}C$ and $\delta^{15}N$ values of abovementioned sources are summarized in Table S2. In this study, a Bayesian mixing model was applied to confirm that the terrestrial organic matter dominated (79%) in the upper bay (Figure 7A). Although the higher nutrient occurred in the upper bay, the Chl *a* (1.65) was lower and the Bayesian mixing model showed that the contribution of marine organic matter and freshwater phytoplankton was only 8% and 13% (Figure 7A). We

TABLE 2 Summary of the mean values of temperature (T), salinity (S), nutrients (NO_3, NO_2, NH_4^-, PO_4^{3-}), DO, Chl *a*, TSM, POC, PN, POC%, PN%, $\delta^{13}C$, $\delta^{15}N$, C/N, POC/Chl *a*, DOC, a_{254}, a_{325}, $S_{275\text{-}295}$, $SUVA_{254}$, C1, C2, C3, HIX, BIX and FI values in the upper and outer bay of Tieshangang Bay.

	T (°C)	S	NO_3^- (μmol L^{-1})	NO_2^- (μmol L^{-1})	NH_4^+ (μmol L^{-1})	PO_4^{3-} (μmol L^{-1})	AOU (mg L^{-1})	Chl *a* (μg L^{-1})
Upper bay	25.43 ± 0.38	31.33 ± 0.27	5.97 ± 1.80	0.78 ± 0.19	1.82 ± 0.47	0.48 ± 0.22	0.97 ± 0.23	1.65 ± 0.37
Outer bay	25.18 ± 1.08	31.71 ± 0.10	1.28 ± 0.92	0.23 ± 0.09	0.86 ± 0.19	0.09 ± 0.05	0.06 ± 0.49	1.83 ± 0.65
	TSM (mg L^{-1})	POC (mg L^{-1})	PN (mg L^{-1})	POC%	PN%	$\delta^{13}C$ (‰)	$\delta^{15}N$ (‰)	C/N
Upper bay	23.24 ± 6.32	0.45 ± 0.08	0.05 ± 0.02	1.98 ± 0.27	0.20 ± 0.02	-25.3 ± 0.8	3.6 ± 1.2	11.81 ± 1.39
Outer bay	21.30 ± 3.46	0.52 ± 0.13	0.05 ± 0.01	2.54 ± 0.86	0.25 ± 0.08	-25.2 ± 1.0	6.9 ± 0.9	11.96 ± 1.33
	POC/Chl *a*	DOC (mgL^{-1})	a_{254} (m^{-1})	a_{325} (m^{-1})	$S_{275\text{-}295}$(μm^{-1})	$SUVA_{254}$ (m^2 g^{-1} C)	C1 (10^{-2} RU)	C2 (10^{-2} RU)
Upper bay	279.08 ± 54.35	0.78 ± 0.17	3.27 ± 0.88	0.84 ± 0.24	21.65 ± 0.64	1.82 ± 0.46	10.00 ± 1.32	6.88 ± 0.98
Outer bay	308.93 ± 83.14	0.75 ± 0.28	2.58 ± 0.61	0.63 ± 0.14	23.21 ± 0.78	1.61 ± 0.40	8.80 ± 2.27	4.89 ± 1.69
	C3 (10^{-2} RU)	HIX	BIX	FI				
Upper bay	5.16 ± 0.47	2.68 ± 0.17	1.12 ± 0.02	2.53 ± 0.03				
Outer bay	5.63 ± 0.83	1.94 ± 0.30	1.29 ± 0.11	2.53 ± 0.04				

realized there may exist some other uncertainties influencing the estimation of potential POM source, such as the decomposition process. The decomposition of POM can modify the isotopic compositions of POM. However, previous studies indicated that the decomposition of OM has a virtually negligible change on $\delta^{13}C$ (~1‰) (Gearing et al., 1984; Chen et al., 2021). Thus, the isotopic compositions of POM can be used to identify source in the Tieshangang Bay due to the negligible isotopic modification by the POM decomposition. Moreover, although it is difficult to accurately calculate the potential POM source, we believe that the quantification in this study can at least reflect the potential POM source at a large extent.

In contrast, higher POC and PN contents (POC: 0.52 ± 0.13 mg L^{-1}; PN: 0.05 ± 0.01 mg L^{-1}) and enhanced POC% and PN% of the TSM were found in the outer bay (Table 2). The significant positive relationships between POC versus Chl *a* ($p< 0.01$, n = 15) and PN versus Chl *a* ($p< 0.01$, n = 15) suggest that POM is mainly related to *in situ* phytoplankton primary production (Figure S3) (Krishna et al., 2018; Lu et al., 2022). Additionally, lighter ^{12}C and ^{14}N isotopes can be uptaked and removed preferentially during thermodynamic and physiological processes (Li et al., 2021; Lu et al., 2022). Therefore, the slightly increased $\delta^{13}C$ (-25.2 ‰) and enriched $\delta^{15}N$ (6.9‰) found in the outer bay also supported the above inference (Figures 3G, H). Previous studies show that the slow water exchange rate were caused by the semi-enclosed topography, weak local sea currents, and diurnal tides in Tieshangang Bay (Jiang et al., 2017). Therefore, the terrigenous input may decrease seaward (Chen et al., 2022a). Increased Chl *a* level (1.83 μg L^{-1}) in the outer bay were triggered by the reduced turbidity in Tieshangang Bay (Qiu et al., 2019; Chen et al., 2021). As shown in the Figure 7B, Bayesian mixing model showed that the contribution of freshwater phytoplankton (from 13% to 20%) and marine organic matter (from 8% to 12%) increased seaward, since the primary production of OM is mainly supported by the phytoplankton in the seawater.

4.2 POM decomposition dominates the net addition of DOM in the weak dynamic upper bay

High salinity (> 31) and FI (> 1.9) were found in the upper bay, indicating that aquatic organism activity (phytoplankton production or bacterial transformation) dominated DOM sources in the upper bay (Li et al., 2022b; Jiang et al., 2021) (Figures 2B, 5F). This is quite different from the POM in the upper bay, which is mainly derived from terrestrial input. Based on the theoretically conservative mixing lines, remarkable net additions of DOC, CDOM and FDOM into the upper bay were found (Figure 6). A two end-member mixing model revealed that the average net values (Δ) of DOM were 0.12 mg L^{-1} (ΔDOC), 0.32 m^{-1} (Δa_{254}), 0.05 m^{-1} (Δa_{325}), 1.07×10^{-2} RU (ΔC1), 1.05×10^{-2} RU (ΔC2) and 0.35×10^{-2} RU (ΔC3) in the upper bay. Synchronously, the nutrients were also nonconservative, with 0.72 μmol L^{-1} and 0.06 μmol L^{-1} additions for

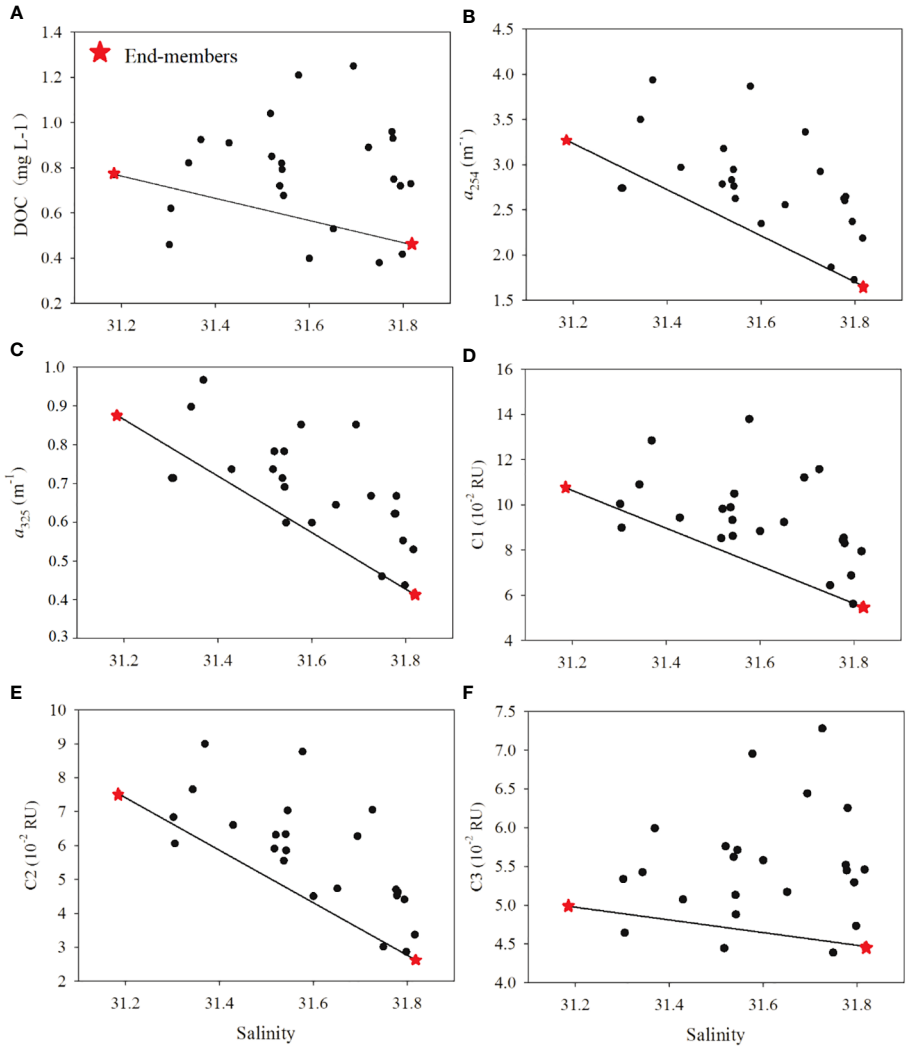

FIGURE 6
Variations of **(A)** DOC (mg L^{-1}), **(B)** a_{254} (m^{-1}), **(C)** a_{325} (m^{-1}), **(D)** C1 (10^{-2} RU), **(E)** C2 (10^{-2} RU), and **(F)** C3 (10^{-2} RU) along with salinity in the water of Tieshangang Bay. The red stars denote the low-salinity and high-salinity end-members used in this study.

NO_3^- and NO_2^-, respectively (Figure 8). Generally, DOM in marine environments might be produced by particle desorption, the release of phytoplankton production, OM decomposition, in addition to allochthonous input (Guo et al., 2014; Hu et al., 2022);. The CDOM contents in the surface layers were similar to those in the bottom layers (such as T3, T4 and T6, depths > 10 m); however, the TSM concentrations in the surface layers were much lower than those in the bottom layers at these stations (Table S1). The lack of correlations between DOM and TSM parameters demonstrated that the direct desorption and dissolution of particles had less impact on DOM in the upper bay (Li et al., 2019; Sun et al., 2022). Both the original DOM parameters (DOC, CDOM, FDOM) and their Δ values were not related to Chl *a* ($p > 0.05$), suggesting that *in situ* phytoplankton primary production was also not the major factor responsible for the net addition of DOM in the upper bay. The lower BIX (average of 1.12 ± 0.02) (*t*-test, $p < 0.001$) also supported the above inference. Abundant terrigenous OM in the marine environments would increase the turbidity of seawater; although higher nutrient was found in the upper bay, the increase in the turbidity of seawater would not be conducive to the growth of phytoplankton in this area. In fact, based on the average net values (Δ) and the original values, the net additions of C3 produced by phytoplankton contributed 7% to the original C3 pool of the upper bay. Therefore, high turbidity may limit the phytoplankton growth, and the primary production may have a weak influence on the addition of DOM.

The dramatic addition of DOC occurred in the upper bay and showed a magnitude comparable to that of CDOM and FDOM. It is therefore believed that the decomposition of DOM would not occur in the upper bay. In summary, we inferred that the microbial-mediated decomposition of terrestrial POM might be the major process that resulted in the net additions of DOC, CDOM and FDOM in the upper bay. The high POC/Chl *a* (>200) indicated that the decomposition of POM occurred in the upper bay (Figure 9) (Cifuentes and Fogel, 1988; Bardhan et al., 2014; Guo et al., 2015; Gawade et al., 2018). Notably, the original a_{325} was not related to

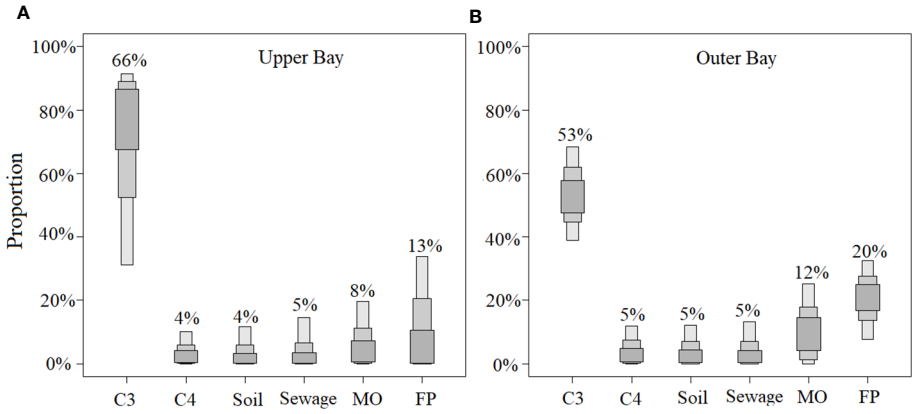

FIGURE 7
POM source contributions in the upper bay **(A)** and outer bay **(B)** of Tieshangang Bay. Soils is terrestrial soil organic matter, MO is marine organic matter, and FP is freshwater phytoplankton; terrigenous organic matter including C3, C4, soil, sewage.

DOC in the upper bay ($p > 0.05$), while Δa_{325} was significantly correlated with ΔDOC. This relationship further supported the above inference that the net addition of DOC and CDOM in the upper bay was mainly subjected to the decomposition of POM. Previous studies have confirmed that humic-like fluorescence increases during microbial decomposition incubations and microbial decomposition is therefore the main sink of humic-like (Wang et al., 2021b). Obviously, the decomposition process contributed 11% and 15% to the original C1 and C2 pools in the upper bay, respectively, which was consistent with the higher HIX in the upper bay. The coastal diluted water discharges might have carried more domestic sewage or bacteria into the sea (Lao et al., 2019; Lu et al., 2021; Mattioli et al., 2016); this process can result in water deterioration and POM decomposition. Previous studies have demonstrated that bacterial activity is a crucial factor that influences the composition of DOM and relates the conversion of POM to DOM. (Kaiser and Benner, 2008). In the northern Beibu Gulf, He et al. (2019) showed that the heterotrophic bacteria abundance of

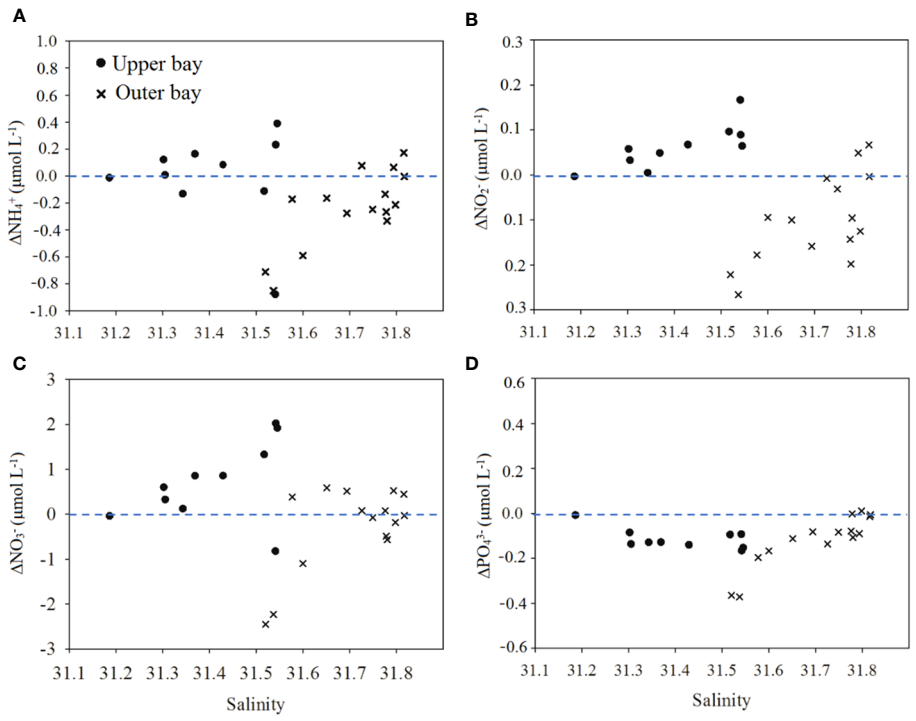

FIGURE 8
Relationships between **(A)** salinity and offset- NH_4^+, **(B)** salinity and ΔNO_2^-, **(C)** salinity and ΔNO_3^-, and **(D)** salinity and ΔPO_4^{3-} in the water column (upper bay and outer bay) of Tieshangang Bay. ΔNH_4^+, ΔNO_2^-, ΔNO_3^-, and ΔPO_4^{3-} are the differences between the observed and expected values, obtained from the end-member mixing model.

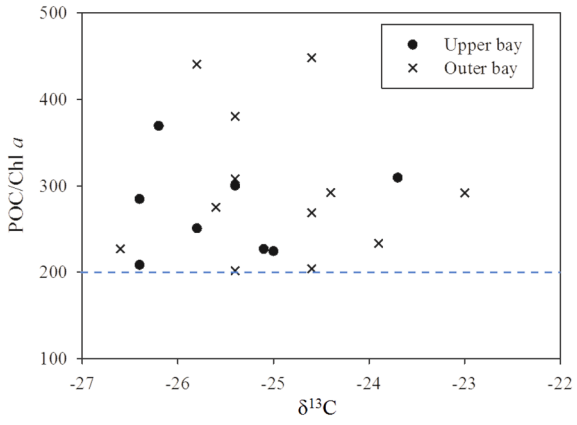

FIGURE 9
$\delta^{13}C$ and POC/Chl *a* ratios in the water column of Tieshangang Bay.

$(11.01 \pm 6.31) \times 10^5$ cell/mL, and He et al. (2022b) demonstrate that heterotrophic bacteria abundance of 12.61×10^5 cell/mL in the seawater; moreover, these studies suggested that the heterotrophic bacteria are densely distributed in the coastal water, and gradually reduce in the offshore. (He et al., 2019; He et al., 2022b). These further confirmed strong bacterial decomposition of POM. The hydrodynamic conditions are very weak due to very small runoff flowing into Tieshanggang Bay. Therefore, the tide controls the water exchange and results in the long water residence time in the upper bay (Jiang et al., 2017). Such hydrological features offered a good opportunity for full microbial decomposition of POM and caused the accumulation of additional DOM in the upper bay but not exported to the outer bay over time.

4.3 The enhanced primary production and decomposition of autochthonous POM jointly contribute to the net addition of DOM in the outer bay

The CDOM (a_{254} and a_{325}) decreased seaward. In addition, the original CDOM coefficients (a_{254} and a_{325}) were positively related with the Chl *a* concentrations ($p< 0.05$, n = 15), indicating that DOM and POM may share the same source (i.e., phytoplankton production). Similar to DOM in the upper bay, the nonconservative behaviors of DOM in the outer bay were also profound. The average net values (Δ) of DOM were 0.23 mg L^{-1} (ΔDOC), 0.64 m^{-1} (Δa_{254}), 0.13 m^{-1} (Δa_{325}), 2.38×10^{-2} RU (ΔC1), 1.39×10^{-2} RU (ΔC2) and 1.06×10^{-2} RU (ΔC3) in the outer bay.

For the decomposition of POM, the POC/Chl *a* ratio raised from 279.08 in the upper bay to 308.93 in the outer bay, suggesting that POM decomposition was more intense than in the upper bay. The higher Chl *a* value, POC% and PN% of the TSM, slightly increased $\delta^{13}C$ (-25.2 ‰) and enriched $\delta^{15}N$ (6.9 ‰) confirmed that the increase of *in situ* phytoplankton production contributes greatly to POM in the outer bay. Previous studies suggested that the newly produced POM preferentially decomposed in the water column (Cifuentes and Fogel, 1988; Guo et al., 2015). Therefore, the abundance of fresh POM (i.e., fresh Chl *a*) is conducive to the heterotrophic process of bacteria in the outer bay. Additionally, the long water residence time provides good conditions for bacterial activity in the outer bay (Jiang et al., 2017; Chen et al., 2022a). As shown in Figure 10, the FDOM exhibited more positive Δ values in the outer bay, that is, the net values (Δ) of C1 were 2.2 times higher and the net values (Δ) of C2 were 1.3 times higher than those in the upper bay. Additionally, the decomposition process contributed 27% to the original C1 pool and 28% to the original C2 pool of the outer bay. These results also suggested that the more intense decomposition of POM occurred due to the freshly produced POM in the outer bay.

The positive net values (Δ) of C3 were 3.0 times higher than those in the upper bay, and this phenomenon may be related to phytoplankton-derived DOM. Phytoplankton production was considered to be one of the most important biogeochemical driver of DOM fluctuation in seawater. Therefore, the generation and accumulation of labile DOM (protein-like C3) were found in this highly productive region, consistent with the higher $S_{275\text{-}295}$ and lower $SUVA_{254}$ in the outer bay. Additionally, the positive net values (Δ) of C3 produced by phytoplankton contributed 19% to the original C3 pool of the outer bay, also confirming the increased contribution of primary production. Although decomposition of POM still occurred in the outer bay, unlike what was found in the upper bay, the nutrient decreased, and more nutrients showed a negative net (Δ) value in the outer bay (Figure 8), indicating that phytoplankton uptake affects nutrient levels in the outer bay. Phytoplankton growth in the outer bay is triggered by nutrient input from the decomposition of POM and reduced turbidity in the water column. Therefore, Chl *a* was the one of the most significant biogeochemical drivers of protein-like C3 fluctuation in the outer bay (Letourneau and Medeiros, 2019; Bowen et al., 2019; Chiranjeevulu et al., 2014; Loginova et al., 2016). Despite the decomposition of POM and the concomitant production of

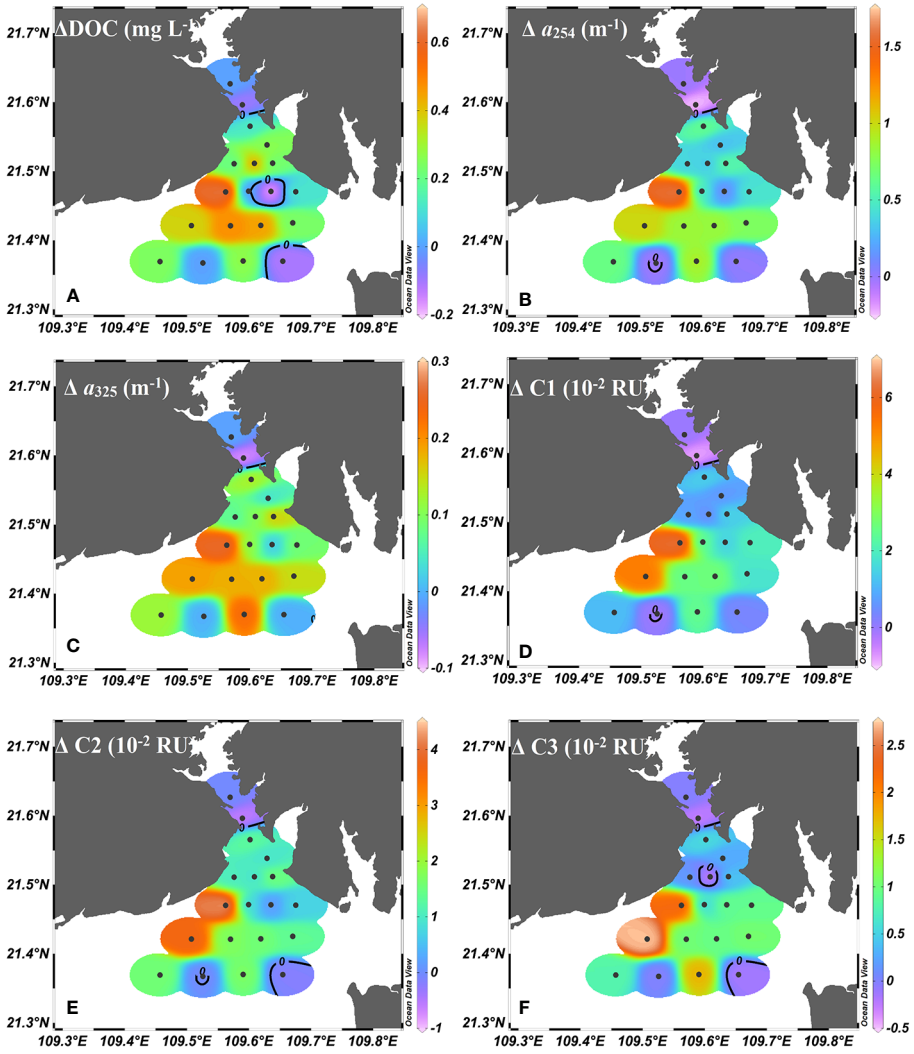

FIGURE 10
Net **(A)** DOC values (ΔDOC), **(B)** a_{254} values (Δa_{254}), **(C)** a_{325} values (Δa_{325}), **(D)** C 1 values (ΔC1), **(E)** C2 values (ΔC2), and **(F)** C3 values (ΔC3) in the water of Tieshangang Bay.

humic-like FDOM in the outer bay, however, the decrease in HIX indices ranged from 1.38 to 2.41, with an average of 1.94 ± 0.30, and the increase in BIX values varied from 1.13 to 1.54, with an average of 1.29 ± 0.11, all suggesting that they were connected with increasing autochthonous biological activity. Therefore, our data suggested that elevated primary production would have an important impact on the DOM pool in the outer bay.

Generally, protein-like are representative of the dynamics of the labile DOM pool, while humic-like materials can be produced as a byproduct of microbial DOM decomposition (Wang et al., 2021a; Wang et al., 2021b). In this study, the increase in protein-like C3 occurred in the outer bay, and the components were labile and linked to primary production in the water. This phenomenon suggested that the decomposition of POM was more intense than the decomposition of protein-like C3, as evidenced by the increased BIX values in the outer bay. Therefore, comparing with the upper bay, the addition of DOM was mainly caused by the decomposition of freshly produced POM (i.e., fresh Chl *a*) and planktonic production in the outer bay.

4.4 Implications for organic carbon circulation in the weak hydrodynamic bay

The sources and biogeochemistry of POM or DOM have been reported separately (Tremblay et al., 2015; Karlsson et al., 2016; Ke et al., 2020; Chen et al., 2021). However, few studies combined the indices of POM and DOM to systematically explore the sources and biogeochemical behaviors of OM (Qu et al., 2022);. The summary of the OM cycle in the Tieshangang Bay is presented in Figure 11. Overall, the weak hydrodynamics promoted a strong decomposition process that controlled the biogeochemistry of POM and DOM across the Tieshangng Bay, southern China, which provide a new

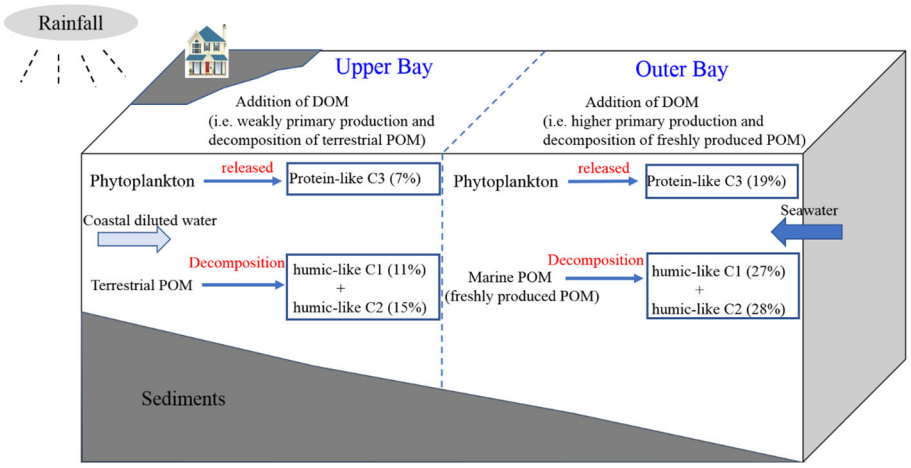

FIGURE 11
A brief diagram of the OM cycle in Tieshangang Bay.

insight of the carbon and nitrogen cycle in a coastal bay. In many coastal areas of the world, the circumstance, i.e., heterotrophy over autotrophy, not only causes water hypoxia and therefore deteriorates the marine ecosystem but also emits CO_2 through OM decomposition (Gawade et al., 2018) and generates positive feedback on global climate change (Laruelle et al., 2010; Wang et al., 2021a; Wang et al., 2021b; Hu et al., 2022). Moreover, the degradation processes of POM and DOM can be further explored with field culture experiments in in the future. Currently, global warming has caught people's attention; thus, it is essential necessary to understand C and N cycling and step toward effective coastal management.

5 Conclusion

By analyzing the $\delta^{13}C$ and $\delta^{15}N$ of POM, absorption and fluorescence of DOM, together with conventional geochemical indicators, the origin, distribution, and fate of POM and DOM was studies in Tieshangang Bay, a weak dynamic bay in the early rainy season. In the upper bay, POM source was mainly originated from terrestrial input, however, external aquatic organism activity dominated DOM sources. In contrast, considerable contributions of the *in situ* biological activities to OM in the outer bay. DOM did not show conservative mixing behavior in Tieshangang Bay, with net additions of DOC and optical components of DOM in both the upper and outer bays. The decomposition of terrestrial POM was the primary factor responsible for the additions of DOM in the upper bay, whereas the enhanced primary production and the strong decomposition of freshly produced POM jointly contributed to the net addition of DOM in the outer bay. Overall, the weak hydrodynamics promoted a strong decomposition process that controlled the biogeochemistry of POM and DOM across the Tieshangng Bay, southern China.

Data availability statement

The datasets presented in this study can be found in online repositories. The names of the repository/repositories and accession number(s) can be found in the article/Supplementary Material.

Author contributions

FC: Conceptualization, Funding acquisition. XL and QL: Writing-Original draft, Data Curation, Visualization, Software. XL and CW: Formal analysis. XL, QL, GJ, and CC: Investigation. CC: Methodology. FC: Project administration, Resources. FC: Supervision, Validation. FC, CW, QL, GJ, XZ, and XL: Writing-Review and Editing. All authors contributed to the article and approved the submitted version.

Funding

This study was supported by the National Natural Science Foundation of China (U1901213, 92158201), Guangdong Natural Science Foundation of China (2019B1515120066), Inovation and Entrepreneurship Project of Shantou (2021112176541391) and Guangxi Natural Science Foundation of China (2020GXNSFBA297065).

Acknowledgments

We would like to thank Marine Environmental Monitoring Centre of Beihai, State Oceanic Administration, for their assistance with collecting water samples.

Conflict of interest

The authors declare that the research was conducted in the absence of any commercial or financial relationships that could be construed as a potential conflict of interest.

Publisher's note

All claims expressed in this article are solely those of the authors and do not necessarily represent those of their affiliated organizations, or those of the publisher, the editors and the reviewers. Any product that may be evaluated in this article, or claim that may be made by its manufacturer, is not guaranteed or endorsed by the publisher.

Supplementary material

The Supplementary Material for this article can be found online at: https://www.frontiersin.org/articles/10.3389/fmars.2023.1144818/full#supplementary-material

References

Akcay, I., Tugrul, S., and Ozhan, K. (2022). Effects of river inputs on particulate organic matter composition and distributions in surface waters and sediments of the mersin bay, northeastern Mediterranean Sea. *Regional Stud. Mar. Sci.* 52, 102316. doi: 10.1016/j.rsma.2022.102316

Bardhan, P., Karapurkar., S. G., Shenoy., D. M., Kurian., S., and Naqvi., S. (2014). Carbon and nitrogen isotopic composition of suspended particulate organic matter in zuari estuary, west coast of India. *J. Mar. Syst.* 141, 90–97. doi: 10.1016/j.jmarsys.2014.07.009

Bianchi, T. S. (2011). The role of terrestrially derived organic carbon in the coastal ocean: A changing paradigm and the priming effect. *Proc. Natl. Acad. Sci. U. S. A.* 108 (49), 19473–19481. doi: 10.1002/lno.11244

Blair, N. E., and Aller, R. C. (2012). The fate of terrestrial organic carbon in the marine environment. *Annu. Rev. Mar. Sci.* 4, 401–423. doi: 10.1146/annurev-marine-120709-142717

Bowen, J. C., Kaplan, L. A., and Cory, R. M. (2019). Photodegradation disproportionately impacts biodegradation of semi-labile DOM in streams. *Limnol. Oceanogr.* 65, 1–14. doi: 10.1002/lno.11244

Chen, Y., Hu, C., Yang, G. P., Gao, X., and Zhou, L. M. (2020). Variation and reactivity of organic matter in the surface sediments of the changjiang estuary and its adjacent East China Sea. *J. Geophys. Res.: Biogeosci.* 126, e2020JG005765. doi: 10.1029/2020JG005765

Chen, C. Q., Lao, Q. B., Shen, Y. L., Jin, G. Z., Chen, F. J., Su, Q. Z., et al. (2022a). Comparative study of nitrogen cycling between a bay with riverine input and a bay without riverine input, inferred from stable isotopes. *Front. Mar. Sci.* 9. doi: 10.3389/fmars.2022.885037

Chen, X., Liu, J., Chen, J., Wang, J., Xiao, X., He, C., et al. (2022b). Oxygen availability driven trends in DOM molecular composition and reactivity in a seasonally stratified fjord. *Water Res.* 220, 118690. doi: 10.1016/j.watres.2022.118690

Chen, F. J., Lu, X., Song, Z. G., Huang, C., Jin, G. Z., Chen, C. Q., et al. (2021). Coastal currents regulate the distribution of the particulate organic matter in western guangdong offshore waters as evidenced by carbon and nitrogen isotopes. *Mar. pollut. Bull.* 172, 112856. doi: 10.1016/j.marpolbul.2021.112856

Chiranjeevulu, G., Murty, K. N., Sarma, N. S., Kiran, R., Chari, N, V, H, K., Pandi, S. R., et al. (2014). Colored dissolved organic matter signature and phytoplankton response in a coastal ecosystem during mesoscale cyclonic (cold core) eddy. *Mar. Environ. Res.* 98, 49–59. doi: 10.1016/j.marenvres.2014.03.002

Cifuentes, L. A., and Fogel, S. (1988). Stable carbon and nitrogen isotope biogeochemistry in the Delaware estuary. *Limnol. Oceanogr.* 33, 1102–1115. doi: 10.4319/lo.1988.33.5.1102

Coble, P. G. (1996). Characterization of marine and terrestrial DOM in seawater using excitation-emission matrix spectroscopy. *Mar. Chem.* 51, 325–346. doi: 10.1016/0304-4203(95)00062-3

Cory, R. M., and Mcknight, D. M. (2005). Fluorescence spectroscopy reveals ubiquitous presence of oxidized and reduced quinones in DOM. *Environ. Sci. Technol.* 39, 8142–8149. doi: 10.1021/es0506962

Dan, S. F., Cui, D., Yang, B., Wang, X., Ning, Z., Lu, D., et al. (2022). Sources, burial flux and mass inventory of black carbon in surface sediments of the daya bay, a typical mariculture bay of China. *Mar. pollut. Bull.* 179 (5-12), 113708. doi: 10.1016/j.marpolbul.2022.113708

Gan, H., Lin, J., Liang, K., and Xia, Z. (2013). Selected trace metals (As, cd and Hg) distribution and contamination in the coastal wetland sediment of the northern beibu gulf, south China Sea. *Mar. pollut. Bull.* 66 (1-2), 252–258. doi: 10.1016/j.marpolbul.2012.09.020

Gao, X. F., Chen, H. H., Gu, B. H., Jeppesen, E., Xue, Y. Y., and Yang, J. (2021b). Particulate organic matter as causative factor to eutrophication of subtropical deep freshwater: Role of typhoon (tropical cyclone) in the nutrient cycling. *Water Res.* 188, 116470. doi: 10.1016/j.watres.2020.116470

Gao, L., Gao, Y., Zong, H., and Guo, L. (2019). Elucidating the hidden nonconservative behavior of DOM in large river-dominated estuarine and coastal environments. *J. Geophys. Res.: Oceans* 124, 4258–4271. doi: 10.1029/2018JC014731

Gao, C., Yu, F., Chen, J., Huang, Z., and Zong, Y. (2021a). Anthropogenic impact on the organic carbon sources, transport and distribution in a subtropical semi-enclosed bay. *Sci. Total Environ.* 767, 145047. doi: 10.1016/j.scitotenv.2021.145047

Gawade, L., Krishna, M. S., Sarma, V. V. S. S., Hemalatha, K. P. J., and Rao, Y. V. (2018). Spatio-temporal variability in the sources of particulate organic carbon and nitrogen in a tropical godavari estuary. *Estuar. Coast. Shelf Sci.* 215, 20–29. doi: 10.1016/j.ecss.2018.10.004

Gearing, J. N., Gearing, P. J., Rudnick, D. T., Requejo, A. G., and Hutchins, M. J. (1984). Isotopic variability of organic carbon in a phytoplankton-based, temperate estuary. *Geochim. Cosmochim. Acta* 48, 1089–1098. doi: 10.1016/0016-7037(84)90199-6

Guo, W., Yang, L., Zhai, W. D., Chen, W. Z., Osburn, C. L., Huang, X., et al. (2014). Runoff-mediated seasonal oscillation in the dynamics of dissolved organic matter in different branches of a large bifurcated estuary–the changjiang estuary. *J. Geophys. Res.: Biogeosci.* 119, 7 7 6–7 793. doi: 10.1002/2013JG002540

Guo, W., Ye, F., Xu, S., and Jia, G. D. (2015). Seasonal variation in sources and processing of particulate organic carbon in the pearl river estuary, south China. *Estuar. Coast. Shelf Sci.* 167, 540–548. doi: 10.1016/j.ecss.2015.11.004

He, D., Li, P. H., He, C., Wang, Y. T., and Shi, Q. (2022a). Eutrophication and watershed characteristics shape changes in dissolved organic matter chemistry along two river-estuarine transects. *Water Res.* 214, 118196. doi: 10.1016/j.watres.2022.118196

He, W. D., Sun, P. F., and Zhang, Q. F. (2022b). Spatial distribution characteristics and influencing factors of planktonic bacteria in the northern beibu gulf in summer. *J. Shanghai Ocean Univ.* 31 (2), 433–444. doi: 10.12024/jsou.20210203286

He, C., Xu, S., Song, S. Q., and Li, C. W. (2019). Spatial-temporal distribution of heterotrophic bacteria in seawater of the northern beibu gulf. *Haiyang Xuebao.* 41 (4), 94–108. doi: 10.3969/j.issn.0253-4193.2019.04.009

Hedges, J. I., Keil, R. G., and Benner, R. (1997). What happens to terrestrial organic matter in the ocean. *Organ. Geochem.* 27, 195–212. doi: 10.1016/S0146-6380(97)00066-1

Helms, J. R., Stubbins, A., Ritchie, J. D., Minor, E. C., Kieber, D. J., and Mopper, K. (2008). Absorption spectral slopes and slope ratios as indicators of molecular weight, source, and photobleaching of chromophoric dissolved organic matter. *Limnol. Oceanogr.* 53 (3), 955–969. doi: 10.4319/lo.2008.53.3.0955

Hu, B., Wang, P., Wang, C., and Bao, T. (2022). Photogeochemistry of particulate organic matter in aquatic systems: A review. *Sci. Total Environ.* 806, 150467. doi: 10.1016/j.scitotenv.2021.150467

Huang, C., Chen, F., Zhang, S., Chen, C., Meng, Y., Zhu, Q., et al. (2020). Carbon and nitrogen isotopic composition of particulate organic matter in the pearl river estuary and the adjacent shelf. *Estuarine Coast. Shelf Sci.* 246, 107003. doi: 10.1016/j.ecss.2020.107003

Huguet, A., Vacher, L., Relexans, S., Saubusse, S., Froidefond, J. M., and Parlanti, E. (2009). Properties of fluorescent dissolved organic matter in the gironde estuary. *Organic Geochem.* 40 (6), 706–719. doi: 10.1016/j.orggeochem.2009.03.002

Jiang, C., Liu, Y., Long, Y., and Wu, C. (2017). Estimation of residence time and transport trajectory in tieshangang bay, China. *Water* 9 (5), 321. doi: 10.3390/w9050321

Jiang, M., Sheng, Y. Q., Tian, C. G., LI, C. Y., Liu, Q. Q., and Li., Z. R. (2021). Feasibility of source identification by DOM fingerprinting in marine pollution events. *Mar. pollut. Bull.* 173, 113060. doi: 10.1016/j.marpolbul.2021.113060

Kaiser, K., and Benner, R. (2008). Major bacterial contribution to the ocean reservoir of detrital organic carbon and nitrogen. *Limnol. Oceanogr.* 53 (1), 99–112. doi: 10.4319/lo.2008.53.1.0099

Kaiser, D., Daniela, U., Qiu, G. L., Zhou, H. L., and Gan, H. Y. (2013). Natural and human influences on nutrient transport through a small subtropical Chinese estuary. *Sci. Total Environ.* 450-451, 92–107. doi: 10.1016/j.scitotenv.2013.01.096

Karlsson, E., Gelting, J., Tesi, T., Dongen, B. V., Andersson, A., Semiletov, I., et al. (2016). Different sources and degradation state of dissolved, particulate, and sedimentary organic matter along the Eurasian Arctic coastal margin. *Global Biogeochem. Cycles* 30, 898–919. doi: 10.1002/2015GB005307

Ke, Z., Chen, D., Liu, J., and Tan, Y. (2020). The effects of anthropogenic nutrient inputs on stable carbon and nitrogen isotopes in suspended particulate organic matter in jiaozhou bay, China. *Continental Shelf Res.* 208, 104244. doi: 10.1016/j.csr.2020.104244

Krishna, M. S., Mukherjee, J., Dalabehera, H. B., and Sarma, V. V. S. S. (2018). Particulate organic carbon composition in temperature fronts of the northeastern Arabian Sea during winter. *J. Geophys. Res.: Biogeosci.* 123, 1–16. doi: 10.1002/2018JG004387

Kubo, A., and Kanda, J. (2016). Seasonal variations and sources of sedimentary organic carbon in Tokyo bay. *Mar. pollut. Bull.* 114 (2), 637–643. doi: 10.1016/j.marpolbul.2016.10.030

Lønborg, C., and Álvarez-Salgado, X. (2014). Tracing dissolved organic matter cycling in the eastern boundary of the temperate north Atlantic using absorption and fluorescence spectroscopy. *Deep Sea Res. Part I: Oceanogr. Res. Papers* 85, 35–46. doi: 10.1016/j.dsr.2013.11.002

Lao, Q. B., Chen, F. J., Liu, G. Q., Chen, C. Q., Jin, G. Z., and Zhu, Q. M. (2019). Isotopic evidence for the shift of nitrate sources and active biological transformation on the western coast of guangdong province, south China. *Mar. pollut. Bull.* 142, 603–612. doi: 10.1016/j.marpolbul.2019.04.026

Lao, Q., Zhang, S., Li, Z., Chen, F., Zhou, X., Jin, G., et al. (2022). Quantification of the seasonal intrusion of water masses and their impact on nutrients in the beibu gulf using dual water isotopes. *J. Geophys. Res.: Oceans* 127, e2021JC018065. doi: 10.1029/2021JC018065

Laruelle, G. G., Durr, H. H., Slomp, C. P., and Borges, A. V. (2010). Evaluation of sinks and sources of CO_2 in the global coastal ocean using a spatially-explicit typology of estuaries and continental shelves. *Geophys. Res. Lett.* 37, L15607. doi: 10.1029/2010GL043691.L15607

Letourneau, M. L., and Medeiros, M. P. (2019). Dissolved organic matter composition in a marsh-dominated estuary: Response to seasonal forcing and to the passage of a hurricane. *J. Geophys. Res.: Biogeosci.* 124, 1545–1559. doi: 10.1029/2018JG004982

Li, J. C., Chen, F. J., Zhang, S. W., Huang, C., Chen, C. Q., Zhou, F., et al. (2021). Origin of the particulate organic matter in a monsoon-controlled bay in southern China. *J Mar Sci Eng.* 9, 541. doi: 10.3390/jmse9050541

Li, X., Li, C., Bai., Y., Shi, X. Y., and Su, R. G. (2019). Composition variations and spatiotemporal dynamics of dissolved organic matters during the occurrence of green tide (Ulva prolifera blooms) in the southern yellow Sea, China. *Mar. pollut. Bull.* 146, 619–630. doi: 10.1016/j.marpolbul.2019.07.021

Li, M. T., Song, G. S., and Xie, H. X. (2022a). Bio- and photo-lability of dissolved organic matter in the pearl river (Zhujiang) estuary. *Mar. pollut. Bull.* 174, 113300. doi: 10.1016/j.marpolbul.2021.113300

Li, Y. Z., Zhang, Y., Li, Z., Wang, J., Dang, C. Y., and Fu, J. (2022b). Characterization of colored dissolved organic matter in the northeastern south China Sea using EEMs-PARAFAC and absorption spectroscopy. *J. Sea Res.* 180, 102159. doi: 10.1016/j.seares.2021.102159

Lin, H., Lan, W., Feng, Q., Zhu, X., Li, T., Zhang, R., et al. (2021). Pollution and ecological risk assessment, and source identification of heavy metals in sediment from the beibu gulf, south China Sea. *Mar. pollut. Bull.* 168, 112403. doi: 10.1016/j.marpolbul.2021.112403

Lin, Y. P., Li, Y. H., Zheng, B. X., Yin, X. J., Wang, L., He, J., et al. (2019). Evolution of sedimentary organic matter in a small river estuary after the typhoon process: A case study of quanzhou bay. *Sci. Total Environ.* 686, 290–300. doi: 10.1016/j.scitotenv.2019.05.452

Liu, Q., Liang, Y., Cai, W. J., Wang, K., Wang, J., and Yin, K. (2020a). Changing riverine organic C:N ratios along the pearl river: Implications for estuarine and coastal carbon cycles. *Sci. Total Environ.* 709, 1–10. doi: 10.1016/j.scitotenv.2019.136052

Liu, Y. C., Ye, Q. H., Huang, W. L., Feng, L., Wang, Y. H., Xie, Z., et al. (2020b). Spectroscopic and molecular-level characteristics of dissolved organic matter in the pearl river estuary, south China. *Sci. Total Environ.* 710, 136307. doi: 10.1016/j.scitotenv.2019.136307

Loginova, A. N., Thomsen, S., and Engel., A. (2016). Chromophoric and fluorescent dissolved organic matter in and above the oxygen minimum zone off Peru. *J. Geophys. Res.: Oceans* 121, 7973–7990. doi: 10.1002/2016JC011906

Lorenzen, C. J. (1967). Determination of chlorophyll and pheopigments: Spectrophotometric equations. *Limnol. Oceanogr.* 12, 343–346. doi: 10.4319/lo.1967.12.2.0343

Lu, X., Huang, C., Chen, F. J., Zhang, S. W., Lao, Q B., Chen, C. Q., et al. (2021). Carbon and nitrogen isotopic compositions of particulate organic matter in the upwelling zone off the east coast of Hainan Island, China. *Marine Pollution Bull.* 167 (14), 112349. doi: 10.1016/j.marpolbul.2021.112349

Lu, X., Zhou, X., Jin, G. Z., Chen, F. J., Zhang, S. W., Li, Z. Y., et al. (2022). Biological impact of typhoon wipha in the coastal area of Western guangdong: A comparative field observation perspective. *J. Geophys. Res.: Biogeosci.* 127, e2021JG006589. doi: 10.1029/2021JG006589

Mattioli, M. C., Sassoubre, L. M., Russell, T. L., and Boehm, A. B. (2016). Decay of sewage-sourced microbial source tracking markers and fecal indicator bacteria in marine waters. *Water Res.* 108, 106–114. doi: 10.1016/j.watres.2016.10.066

Meyers, P. A. (1994). Preservation of elemental and isotopic source identification of sedimentary organic matter. *Chem. Geol.* 114, 289–302. doi: 10.1016/0009-2541(94)90059-0

Meyers, P. A. (1997). Organic geochemical proxies of paleoceanographic, paleolimnologic, and paleoclimatic processes. *Organic Geochem.* 27, 213–250. doi: 10.1016/S0146-6380(97)00049-1

Pei, M. F., Hu, J. T., and Gao, J. S. (2019). Study on the response of water exchange capability in tieshan bay in guangxi to the reclamation and monsoon. *Trans. Oceanol. Limnol.* 6, 34–40. doi: 10.13984/j.cnki.cn37-1141.2019.06.004

Qiu, D., Zhong, Y., Chen, Y. Q., Tan, Y. H., Song, X. Y., and Huang, L. M. (2019). Short-term phytoplankton dynamics during typhoon season in and near the pearl river estuary, south China Sea. *J. Geophys. Res.: Biogeoences* 124 (2), 274–292. doi: 10.1029/2018JG004672

Qu, L. Y., He, C., Wu, Z. T., Dahlgren, R. A., Ren, M. X., Li, P. H., et al. (2022). Hypolimnetic deoxygenation enhanced production and export of recalcitrant dissolved organic matter in a large stratified reservoir. *Water Res.* 219, 118537. doi: 10.1016/j.watres.2022.118537

Qu, L., Wu, Y., Li, Y., Stubbins, A., Dahlgren, R. A., Chen, N., et al. (2020). El Niño-driven dry season flushing enhances dissolved organic matter export from a subtropical watershed. *Geophys. Res. Lett.* 47, e2020GL089877. doi: 10.1029/2020GL089877

Sarma, V. V. S. S., Krishna, M. S., Prasad, V. R., Kumar, B. S. K., Naidu, S. A., Rao, G. D., et al. (2014). Distribution and sources of particulate organic matter in the Indian monsoonal estuaries during monsoon. *J. Geophys. Res. Biogeosci.* 119, 2095–2111. doi: 10.1002/2014jg002721

Samantaray, S., and Sanyal, P. (2022). Sources and fate of organic matter in a hypersaline lagoon: A study based on stable isotopes from the Pulicat lagoon, India. *Sci Total Environ.* 807, 150617. doi: 10.1016/j.scitotenv.2021.150617

Stedmon, C. A., and Bro, R. (2008). Characterizing dissolved organic matter fluorescence with parallel factor analysis: A tutorial. *Limnol. Oceanogr.: Methods* 6 (11), 572–579. doi: 10.4319/lom.2008.6.572

Sun, X., Li, P., Zhou, Y., He, C., Cao, F., Wang, Y., et al. (2022). Linkages between optical and molecular signatures of dissolved organic matter along the Yangtze river estuary-toEast China Sea continuum. *Front. Mar. Sci.* 9. doi: 10.3389/fmars.2022.933561

Tremblay, L., Caparros, J., Leblanc, K., and Obernosterer, I. (2015). Origin and fate of particulate and dissolved organic matter in a naturally irn-fertilized region of the southern ocean. *Biogeosciences* 12 (2), 607–621. doi: 10.5194/bg-12-607-2015

Wada, E., and Hattori, A. (1990). *Nitrogen in the Sea: Forms, abundance, and rate processes* (US: CRC-Press).

Wang, C., Guo, W., Li, Y., Dahlgren, R. A., Guo, X., Qu, L., et al. (2021a). Temperature-regulated turnover of chromophoric dissolved organic matter in global dark marginal basins. *Geophys. Res. Lett.* 48, e2021GL094035. doi: 10.1029/2021GL094035

Wang, C., Li, Y., Li, Y., Zhou, H., Stubbins, A., and Dahlgren, R. A. (2021b). Dissolved organic matter dynamics in the epipelagic Northwest pacific low-latitude Western boundary current system: Insights from optical analyses. *J. Geophys. Res.: Oceans* 126, e2021JC017458. doi: 10.1029/2021JC017458

Weishaar, J. L., Aiken, G. R., Bergamaschi, B. A., and Fram, M. S. (2003). Evaluation of specific ultraviolet absorbance as an indicator of the chemical composition and reactivity of dissolved organic carbon. *Environ. Sci. Technol.* 37 (20), 4702–4708. doi: 10.1021/es030360x

Xia, J., Han, Y., Tan, J., Abarike, G. A., and Song, Z. (2022). The characteristics of organic carbon in the offshore sediments surrounding the leizhou peninsula, China. *Front. Earth Sci.* 10. doi: 10.3389/feart.2022.648337

Xu, C., Yang, B., Dan, S. F., Zhang, D., and Peng, S. (2020). Spatiotemporal variations of biogenic elements and sources of sedimentary organic matter in the largest oyster mariculture bay (Maowei Sea), southwest China. *Sci. Total Environ.* 730, 139056. doi: 10.1016/j.scitotenv.2020.139056

Xu, C., Dan, S. F., Yang, B., Lu, D., Kang, Z., Huang, H., et al (2021). Biogeochemistry of Dissolved and Particulate Phosphorus Speciation in the Maowei Sea, Northern Beibu Gulf. *J. Hydrol.* 593, 125822. doi: /10.1016/j.jhydrol.2020.125822

Ye, F., Guo, W., Shi, Z., Jia, G. D., and Gang, J. (2017). Seasonal dynamics of particulate organic matter and its response to flooding in the pearl river estuary, China, revealed by stable isotope ($\delta^{13}C$ and $\delta^{15}N$) analyses. *J. Geophys. Res.: Oceans* 122, 6835–6856. doi: 10.1002/2017JC012931

Zhang, D., Lu, D., Yan, B., Zhang, J., Ning, Z., and Yu, K. (2019). Influence of natural and anthropogenic factors on spatial-temporal hydrochemistry and the susceptibility to nutrient enrichment in a subtropical estuary. *Mar. pollut. Bull.* 146, 945–954. doi: 10.1016/j.marpolbul.2019.07.056

Zhao, C., Zhou, Y. P., Pang, Y., Zhang, Y. Z., Huang, W., Wang, Y. T., et al. (2021). The optical and molecular signatures of DOM under the eutrophication status in a shallow, semi-enclosed coastal bay in southeast China. *Sci. China Earth Sci.* 64 (7), 1090–1104. doi: 10.1007/s11430-020-9728-4

Zhu, Z., Wei, H., Guan, Y., Zhang, L., Sun, P., and Zhang, Q. (2022). Spatial and seasonal characteristics of dissolved heavy metals in the seawater of beibu gulf, the northern south China Sea. *Front. Marine Sci.* 9. doi: 10.3389/fmars.2022.996202

Zsolnay, A., Baigar, E., Jimenez, M., Steinweg, B., and Saccomandi, F. (1999). Differentiating with fluorescence spectroscopy the sources of dissolved organic matter in soils subjected to drying. *Chemosphere* 38 (1), 45–50. doi: 10.1016/S0045-6535(98)00166-0